Continuum effect in resonance spectra of neutron-rich oxygen isotopes*

Si-Jie Dai(戴思捷)[1] Fu-Rong Xu(许甫荣)[1;1)] Jian-Guo Li(李健国)[1]
Bai-Shan Hu(胡柏山)[1] Zhong-Hao Sun(孙中浩)[1,2]

[1] School of Physics, and State Key Laboratory of Nuclear Physics and Technology, Peking University, Beijing 100871, China
[2] Physics Division, Oak Ridge National Laboratory, Oak Ridge, Tennessee 37831, USA

Abstract: Starting from the CD-Bonn potential, we have performed Gamow shell-model calculations for neutron-rich oxygen isotopes, investigating excitation spectra and their resonant properties. The Gamow shell model is based on the Berggren ensemble, which is capable of treating the continuum effect reasonably in weakly bound or unbound nuclei. To calculate heavier-mass oxygen isotopes, we choose ^{16}O as a frozen core in the Gamow shell-model calculations. The first 2^+ excitation energies of the even-even O isotopes are calculated, and compared with those obtained by the conventional shell model using the empirical USDB interaction. The continuum effect is proved to play an important role in the shell evolution near the drip line. We also discuss the effect of the Berggren contour choice. We improve the approximation in the contour choice to give more precise calculations of resonance widths.

Keywords: CD-Bonn interaction, Gamow shell model, drip-line nuclei, Berggren ensemble, continuum, resonance

PACS: 21.60.Cs, 21.30.Fe, 24.30.Gd **DOI:** 10.1088/1674-1137/42/11/114106

1 Introduction

Thanks to the radioactive isotope beam technique, the exploration of the neutron drip line is no longer unachievable. A recent experiment performed at RIKEN-RIBF investigated the extremely neutron-rich nucleus ^{26}O by removing a proton from the radioactive secondary beam of ^{27}F [1]. The decay products, ^{24}O and two neutrons, were observed. This experiment confirmed that ^{24}O is the last bound nucleus of neutron-rich oxygen isotopes, and positioned the ground-state resonance of ^{26}O at about 18 keV above threshold. Another excited state in ^{26}O was also observed at 1.28 MeV, which is believed to be the first 2^+ state [1].

As a powerful method for studying atomic nuclei, including in the medium-mass region, the shell model is very commonly used to investigate oxygen isotopes [2–4]. Shell model calculations using the USDB interaction have been successful in reproducing the observables of *sd*-shell nuclei, such as the binding energies, spectra, and transition rates [5–9]. However, the USDB interaction is constructed in the harmonic oscillator (HO) basis. The HO basis always gives well-localised wave functions of nuclear states. However, these cannot describe the loosely-bound or unbound properties of drip-line nuclei. For the drip-line nucleus ^{26}O, the HO-basis shell-model calculation with the USDB interaction gives a 2^+ excitation energy about 0.8 MeV higher than the experimental data [1]. The three-body model calculations indicate that the two-neutron decay channel may play an important role in the ^{26}O system [10–12].

In the three-body model calculation, the three-body system is selected as ^{24}O+n+n, and the system is correlated by a density-dependent contact pairing interaction. The two-neutron decay channel is taken into account by evolving the initial state, generated by removing a proton from the calculated ground state of the ^{25}F+n+n system, with the Hamiltonian of the three-body system. The Hamiltonian is based on a one-body Woods-Saxon (WS) potential with a finite depth, and the two-body pairing interaction [10–12]. Using a finite-depth one-body potential is crucial for the model, as it allows particle emissions.

The three-body model has been successful in reproducing the first 2^+ state energy of ^{26}O, as the decay channel can couple the bound and continuum single particle (s.p.) states [10–12]. For describing the properties of weakly-bound or unbound nuclei near the drip line, the continuum effect has already been proved to be very important [13–19]. In the three-body model, a phe-

Received 28 July 2018, Published online 26 September 2018
* Supported by the National Key R&D Program of China (2018YFA0404401), the National Natural Science Foundation of China (11320101004, 11575007), the China Postdoctoral Science Foundation (2018M630018), the CUSTIPEN (China-U.S. Theory Institute for Physics with Exotic Nuclei) funded by the U.S. Department of Energy, Office of Science (DESC0009971), and High-performance Computing Platform of Peking University

1) E-mail: frxu@pku.edu.cn

nomenological pairing interaction is applied. As Ref. [11] pointed out, the pairing strength has to be finely tuned to get a precise result. Fitting the pairing strength mixes different effects, like the continuum effect and the three-body force, and the exact contribution from each one cannot be identified. Another problem is that the three-body model cannot give the decay width directly and the method used to calculate the widths is parameter-dependent [11].

To minimize the obscure mixing effects caused by the fitted interaction, as well as to calculate the decay width self-consistently, we revisit the continuum effect in the oxygen isotopes by the Gamow shell model (GSM) [18, 20, 21] with a realistic nuclear force, the CD-Bonn interaction [22]. The GSM is based on the Berggren ensemble, which is composed of s.p. bound states, resonant states and non-resonant continuums [13, 18, 20, 21]. The continuum states in the Berggren ensemble are analytically extended to the complex plain and discretized along a certain contour. The imaginary parts of the resonant s.p. eigen-energies give the resonance widths of the s.p. states. These s.p. widths integrate to the total widths of the many-body system through the shell model. On the other hand, the CD-Bonn potential describes the nucleon-nucleon interaction with high precision within a very wide range. To accelerate the convergence of many-body calculations, the bare CD-Bonn interaction is renormalized using the $V_{\text{low-}k}$ procedure [23]. For the shell-model calculation with a frozen core, we adopt the Q-box folded-diagram perturbation method [24, 25] to construct a realistic effective model-space Hamiltonian, as done in Ref. [21].

As mentioned above, analytically extending the continuum states to the complex plain is essential in the Berggren ensemble, which includes the narrow resonant states, and introduces an additional dimension to describe the resonance width. However, a complex contour requires more discretizing points to reach convergence due to the additional dimension. Since it is believed that the non-resonant continuums mainly couple with bound states through the resonances, and the direct coupling is assumed to be less important, in most models based on the Berggren ensemble, only continuums belonging to the partial waves that include the narrow resonances are extended to the complex plain [18, 20, 21, 26–30]. However the accuracy of this approximation is not yet well tested. In this paper, we will discuss the Berggren contour choice in the oxygen chain by expanding the extended partial waves of continuums from $d_{3/2}$ to all sd partial waves.

In this paper, we perform a realistic-force GSM calculation for the neutron-rich oxygen isotopes, ^{18,20,22,24,25,26}O, to study how the continuum effect affects the shell evolution in the drip-line region, as well as to investigate the continuum effect from the non-resonant continuums of the partial waves without narrow resonances.

2 Theoretical framework

The Berggren ensemble is an s.p. basis specialized for treating the resonance and continuum. The one-body Schrödinger equation in the complex-k space gives the Berggren states,

$$\frac{\mathrm{d}^2u(r)}{\mathrm{d}r^2}=\left(\frac{l(l+1)}{r^2}+\frac{2m}{\hbar^2}V_{\text{WS}}(r)-k^2\right)u(r), \tag{1}$$

where V_{WS} is the WS potential with a spin-orbit coupling,

$$V_{\text{WS}}(r)=-V_0f(r)-4V_{SO}\frac{1}{r}\frac{\mathrm{d}f(r)}{\mathrm{d}r}l\cdot s, \tag{2}$$

and

$$f(r)=-\frac{1}{1+\mathrm{e}^{\frac{r-r_0A^{1/3}}{d}}}. \tag{3}$$

The basis states include bound, resonant and continuum states due to the finite depth of the WS potential. In the present calculations, the parameters of the WS potential are $V_0=45.39$ MeV, $r_0=1.347$ fm, $d=0.70$ fm, and $V_{\text{SO}}=18.2$ MeV. The sd-shell s.p. energies are -5.31 MeV, -3.22 MeV and (1.06-0.09i) MeV for the $0d_{5/2}$, $1s_{1/2}$ bound states and $0d_{3/2}$ resonant orbit, respectively. The values are the same as the universal parameters [31], except that the strength $|V_0|$ is reduced to reproduce the experimental width extracted from ^{17}O [21].

The completeness relation of the Berggren ensemble can be written as

$$\sum_{n\in\{b,d\}}u_n(r,k_n)u_n(r',k_n)+\int_{L^+}\mathrm{d}kv(r,k)v(r',k)=\delta(r-r'), \tag{4}$$

where b and d denote the bound states and decaying resonant states respectively, and L^+ denotes the integral contour of the continuum. The contour lies in the complex plain. Only the narrow resonances enclosed in the contours are included in the summation of Eq. (4), according to Cauchy's integral theorem. Since the orbital angular momentum in the s.p. Hamiltonian is conserved, the contours of different partial waves may differ. For a partial wave that does not contain narrow resonances, a contour lying on the real-momentum axis is widely used.

The effective interaction in the Berggren ensemble is obtained by performing a Q-box folded-diagram perturbation based on the CD-Bonn interaction. The matrix elements, which are given originally in the HO basis, are projected to the Berggren ensemble by overlapping the Berggren basis wavefunctions and those of the HO basis. In the present work, we are using the truncation N_{shell}=22 for the HO basis. The CD-Bonn interaction is renormalized by the $V_{\text{low-}k}$ procedure before projection to the Berggren ensemble. To minimize the induced

three-body force in the $V_{\text{low-}k}$ renormalization, a hard cutoff of $\Lambda = 2.6$ fm^{-1} is chosen. In the Q-box calculation, the starting energy is -6 MeV, which is approximately equal to the average sd-shell s.p. energy of the one-body Woods-Saxon potential.

With the ^{16}O core, the model space of the effective interaction is all the sd-shell orbits including bound states $0d_{5/2}$ and $1s_{1/2}$, the narrow resonant state $0d_{3/2}$, and the $d_{3/2}$ non-resonant continuum states on the complex plain. As mentioned above, a real-momentum continuum contour is commonly adopted for partial waves that do not have a narrow resonance. Because we are also investigating the continuum effect contributed by partial waves that do not have narrow resonances, the results with the different contours of the $s_{1/2}$ and $d_{5/2}$ partial waves are compared. We change these contours from the real-momentum axis to the same as that of the $d_{3/2}$ partial wave. In the calculation, we choose the contour $\{0.0 \to 2.2\}$ (in fm^{-1}) in the real axis and discretize it with 20 discrete points. The complex contour is taken as $\{0.0 \to (0.48-0.20i) \to 0.62 \to 2.2\}$ (in fm^{-1}), with 20 discrete points as well.

3 Calculations and discussion

The excitation energy of the first 2^+ excited state is an indicator of the shell gap in the sd shell. In this paper, we calculate the 2_1^+ excitation energies of oxygen isotopes, shown in Fig. 1. We see that both the CD-Bonn GSM and USDB HO-basis SM calculations give good agreement with experimental 2_1^+ excitation energies. Especially in the well-bound nuclei, ^{18,20,22}O, both calculations reproduce the data well. This indicates that, although based on a realistic force, the effective interaction in the GSM has the same precision for the well-bound systems as the empirical USDB interaction which fits the data of bound nuclei. However, for the 2_1^+ excitation energy in the unbound ^{26}O, the USDB interaction gives 2.11 MeV, which is about 800 keV higher than the experimental data. The CD-Bonn GSM improves the calculation significantly (see Fig. 1). Since the effective interaction in GSM is as precise as the USDB interaction in well-bound nuclei, we can thus conclude that the improvement should be mainly due to the inclusion of the continuum.

The calculated 2^+ excitations of ^{24}O and ^{26}O are lower than the experimental data, which may be partially due to the lackness of the three-body force in the GSM calculations. With increasing number of valence neutrons, the effect of the three-body force becomes significant. In our previous work [21], we proved that the three-body force introduced by the $V_{\text{low-}k}$ process is weak when the hard cutoff of 2.6 fm^{-1} is used. However, the initial three-body force, which is not considered, would have a non-negligible effect for neutron-rich isotopes with a large number of valence neutrons. In work studying the oxygen chain using the ab-initio coupled cluster method [28], with both two-body and three-body interaction derived from chiral effective field theory [33], the initial three-body force has the effect of increasing the excitation energies of the 2^+ states in the even-even O isotopes. Although the 2^+ state of ^{26}O was not calculated in Ref. [28], the direction of this effect should remain the same. That conclusion supports our result that the 2^+ state is lower in energy than the experimental data if no three-body force is considered.

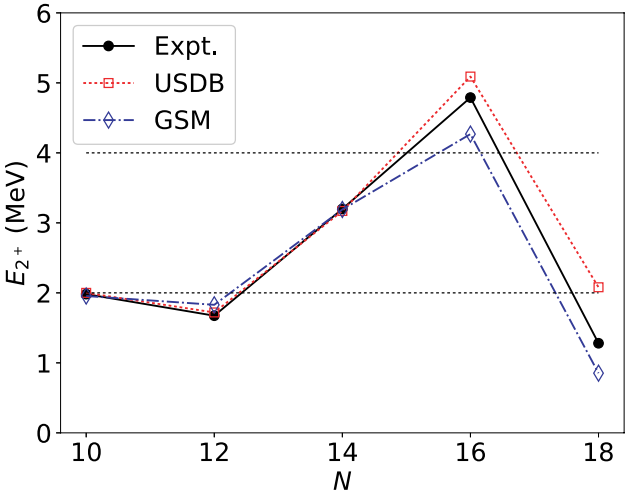

Fig. 1. (color online) The calculated 2_1^+ excitation energies in ^{18,20,22,24,26}O, compared with the experimental data [1, 32] and USDB calculations. The USDB calculation overestimates the 2^+ excitation energy in ^{26}O, while the GSM calculation improves the result by taking the continuum effect into account.

Another purpose of the present work is to investigate the influence of the contour choice. We use the different contours of the sd partial waves to calculate all the well-bound nuclei, and weakly-bound and unbound nuclei. For convenience, we use the following notation:

1) C_0: only the $d_{3/2}$ channel, which contains a narrow resonance, takes a complex contour (i.e. a triangle shape below the real-momentum axis, see Fig. 1 in Ref. [21], our previous paper) with 20 discrete points, while all other channels (including $s_[1/2]$ and $d_{5/2}$ channels), which have no narrow resonances, take real-momentum contours with only 8 discrete points.

2) C_1: same as C_0 except that the number of discrete points for $s_{1/2}$ and $d_{5/2}$ partial waves is increased to 20.

3) C_2: the $s_{1/2}$ channel also takes a complex-momentum contour, like $d_{3/2}$, compared with the C_1 calculations.

4) C_3: both $s_{1/2}$ and $d_{5/2}$ channels take complex-momentum contours, like the narrow-resonance $d_{3/2}$ par-

tial wave, compared with the C_1 calculations.

Figure 2 displays the calculations of low-lying states in $^{22-26}$O. We see that there is not much change in the results when the number of discretizing points is increased from 8 to 20, except in ^{24}O where the energies become slightly lower. An increase in the number of discretizing points leads to a remarkable increase in the model dimension. Therefore, a reasonable but converged number of discretizing points is an issue that one should consider in the GSM calculation. From our calculations for the *sd*-shell nuclei, 8 discretizing points should be reasonable in most cases.

From Fig. 2, we can also analyze the calculations with different strategies of contour choice. Overall, the different strategies in the choices of contours give almost the same results, except that C_3 gives slightly higher energies for the 2^+ and 3^+ states in ^{22}O. This means that for the partial waves with no narrow resonances, real-momentum contours can be chosen without loss of accuracy of the calculations. A real-momentum contour with reasonable discretizing points on it can significantly reduce the computation task. This means that if no narrow resonance is included in the channel, the continuum states on the real-momentum contour are good enough to describe the continuum effect in the real part of the eigen-energies.

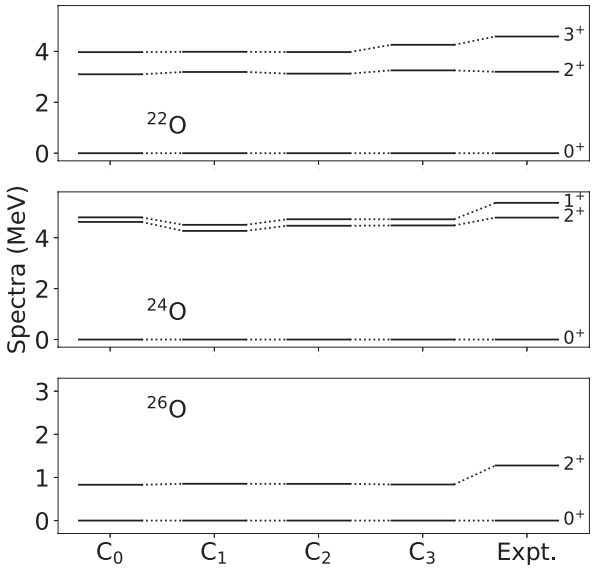

Fig. 2. Calculated low-lying states of ^{22,24,26}O. The experimental data are taken from Refs. [1, 32]. The different strategies of contour choice C_i are defined in the text. The results show that the real parts of the eigen-energies given by GSM calculations do not change meaningfully with the different choices of contours for the channels without narrow resonances.

Figure 3 plots the imaginary parts (i.e., resonance widths) of the obtained eigen-energies of the resonant states in ^{24,25,26}O, compared with the experimental data available currently [1, 32]. The calculated resonance widths are gently dependent on the prescriptions of contour choice. The widths tend to be slightly smaller with more partial waves taking complex-momentum contours, and closer to the experimental values. However, the GSM calculation with a complex-momentum contour is much more expensive in computation. The new experiment on ^{26}O [1] mentioned in the introduction has also updated the resonance width of the unbound ^{25}O ground state. The experimental resonance width of the ^{26}O 2^+ state [1] looks extremely large, much larger than the GSM calculation. In the experiment [1], the experimental strength of the 2^+ resonant state is relatively weak, and the FWHM is influenced a lot by the continuum states around. The present calculation predicts a much smaller resonance width for this state.

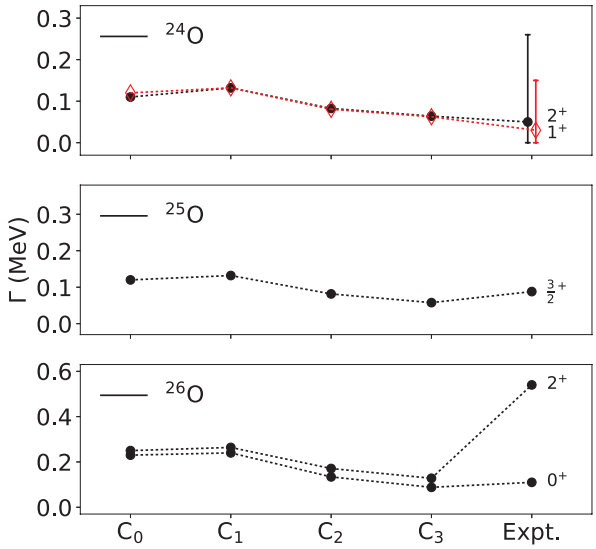

Fig. 3. (color online) Calculated resonance widths of ^{24,25,26}O. The experimental data are taken from Refs. [1, 32].

In the present paper, we are investigating how to treat the continuum effect in both energy and width of the resonance. For the calculation of resonance energy, choosing a real-momentum contour for a partial wave that has no narrow resonance is good enough to give a convergent result. Taking a complex-momentum contour does not change the result. For the calculation of resonance width, however, choosing complex-momentum contours for all partial waves of the model space seems to be more reasonable, and hence recommended. For partial waves belonging to the excluded space, couplings with valence particles are weak, and hence it should be safe to use real-momentum contours for the channels.

4 Conclusion

In conclusion, we have applied the with-core GSM based on the CD-Bonn potential to neutron-rich oxygen isotopes, investigating the continuum effect on both resonance energy and width. These calculations were motivated with the recent experiment on ^{26}O beyond the neutron drip line. The calculated 2^+ excitation energies were compared with shell-model calculations using the empirical USDB interaction, showing a strong continuum effect in the spectra of drip-line nuclei. By choosing the different prescriptions of contours in the Berggren coordinates for the GSM calculation, we have discussed the convergence of the resonance spectrum. It is suggested that all the model-space partial waves, regardless of whether there is a narrow resonance, should take the same complex-momentum contour to obtain a convergent resonance width.

References

1 Y. Kondo and et al, Phys. Rev. Lett., **116**: 102503 (2016)
2 E. Caurier, F. Nowacki, A. Poves and J. Retamosa, Phys. Rev. C, **58**: 2033–2040 (1998)
3 C. R. Hoffman and et al, Phys. Rev. Lett., **100**: 152502 (2008)
4 C. Yuan, T. Suzuki, T. Otsuka, F. Xu, and N. Tsunoda, Phys. Rev. C, **85**: 064324 (2012)
5 B. A. Brown and W. A. Richter, Phys. Rev. C, **74**: 034315 (2006)
6 M. Kowalska and et al, Phys. Rev. C, **77**: 034307 (2008)
7 R. Kanungo and et al, Phys. Rev. Lett., **102**: 152501 (2009)
8 K. Tshoo and et al, Phys. Rev. Lett., **109**: 022501 (2012)
9 S. R. Stroberg, H. Hergert, J. D. Holt, S. K. Bogner, and A. Schwenk, Phys. Rev. C, **93**: 051301 (2016)
10 K. Hagino and H. Sagawa, Phys. Rev. C, **90**: 027303 (2014)
11 K. Hagino and H. Sagawa, Phys. Rev. C, **89**: 014331 (2014)
12 L. V. Grigorenko and M. V. Zhukov, Phys. Rev. C, **91**: 064617 (2015)
13 R. Id Betan, R. J. Liotta, N. Sandulescu, and T. Vertse, Phys. Rev. Lett., **89**: 042501 (2002)
14 K. Bennaceur, J. Dobaczewski, and M. Płoszajczak, Phys. Rev. C, **60**: 034308 (1999)
15 N. Michel, W. Nazarewicz, and M. Płoszajczak, Phys. Rev. C, **82**: 044315 (2010)
16 I. Rotter, Reports on Progress in Physics, **54**(4): 635 (1991)
17 A. Volya and V. Zelevinsky, Phys. Rev. C, **74**: 064314 (2006)
18 N. Michel, W. Nazarewicz, M. Płoszajczak, and K. Bennaceur, Phys. Rev. Lett., **89**: 042502 (2002)
19 W. Fritsch, R. Lipperheide, and U. Wille, Nuclear Physics A, **241**(1): 79–108 (1975)
20 N. Michel, W. Nazarewicz, M. Płoszajczak, and J. Okołowicz, Phys. Rev. C, **67**: 054311 (2003)
21 Z. Sun, Q. Wu, Z. Zhao, B. Hu, S. Dai, and F. Xu. Physics Letters B, **769**: 227–232 (2017)
22 R. Machleidt, Phys. Rev. C, **63**: 024001 (2001)
23 S. Bogner, T. Kuo, and A. Schwenk, Physics Reports, **386**(1): 1–27 (2003)
24 K. Takayanagi, Nuclear Physics A, **852**(1): 61–81 (2011)
25 N. Tsunoda, K. Takayanagi, M. Hjorth-Jensen, and T. Otsuka, Phys. Rev. C, **89**: 024313 (2014)
26 N. Michel, W. Nazarewicz, and M. Płoszajczak, Phys. Rev. C, **70**: 064313 (2004)
27 Y. Jaganathen, R. M. I. Betan, N. Michel, W. Nazarewicz, and M. Płoszajczak, Phys. Rev. C, **96**: 054316 (2017)
28 G. Hagen, M. Hjorth-Jensen, G. R. Jansen, R. Machleidt, and T. Papenbrock, Phys. Rev. Lett., **108**: 242501 (2012)
29 G. Papadimitriou, J. Rotureau, N. Michel, M. Płoszajczak, and B. R. Barrett, Phys. Rev. C, **88**: 044318 (2013)
30 I. J. Shin, Y. Kim, P. Maris, J. P. Vary, C. Forssén, J. Rotureau, and N. Michel, Journal of Physics G: Nuclear and Particle Physics, **44**(7): 075103 (2017)
31 J. Dudek, Z. Szymański, and T. Werner, Phys. Rev. C, **23**: 920–925 (1981)
32 Data extracted using the NNDC On-Line Data Service, http://www.nndc.bnl.gov/
33 R. Machleidt and D. Entem, Physics Reports, **503**(1): 1–75 (2011)